Phase Structures and Phase Diagrams in Polymer Liquid-Crystal Systems: Copolymers of Poly(ethylene terephthalate) and *p*-Hydroxybenzoic acid

Witold Brostow,*,† Michael Hess,†,‡ and Betty L. López†,§

Center for Materials Characterization and Department of Chemistry, University of North Texas, Denton, Texas 76203-5308, FB6-Physikalische Chemie, Universität Duisburg, 47048 Duisburg, Federal Republic of Germany, and Departamento de Química, Facultad de Ciencias Exactas y Naturales, Universidad de Antioquia, Apártado Aéreo 1226, Medellín, Colombia, and Colciencias, Bogotá, Colombia

Received September 30, 1993; Revised Manuscript Received January 19, 1994®

ABSTRACT: The phase diagram of transition temperatures versus the mole fraction x of the liquid-crystalline component PHB was determined for a series of copolymers PET/xPHB, where PET = poly(ethylene terephthalate) and PHB = *p*-hydroxybenzoic acid. The diagram includes both equilibrium and nonequilibrium phases and is based on results reported here as well as on those of earlier investigators and on results obtained by several techniques, with identical samples studied by the same techniques but at different locations. The diagram is fairly complex. The quasi-liquid phase reported earlier is discussed in some detail. The importance of the diagram for intelligent processing is discussed.

1. Introduction

In earlier papers[1,2] we pointed out the importance of the knowledge of phase structures and phase diagrams in polymer liquid crystals (PLCs). PLCs are receiving considerable attention because of fundamental reasons as well as because of their properties desirable in applications.[3-6] PLCs are stronger mechanically than comparable flexible polymers because liquid-crystalline sequences typically exhibit some rigidity. Moreover, PLCs have typically better thermal stability at elevated temperatures, lower thermal expansivity, lower flammability, are stable in vacuum, stable against visible and UV light, and exhibit low melt viscosity in the anisotropic states. The last property makes them considerably easier to process than heterogeneous composites[7,8] such as glass-fiber-reinforced thermoplastics. To develop processability/structure/property relationships, an understanding of phase behavior is indispensable. In 1988 Zachmann and collaborators[9] have shown an example of a PLC phase diagram. In contrast to phase diagrams of non-LC polymer systems, their diagram shows a fairly large number of phase regions and an overall complexity.

One of the first known PLC series were the copolyesters of poly(ethylene terephthalate) (PET) and *p*-hydroxybenzoic acid (PHB), originally synthesized by Jackson and Kuhfuss[10] and designed hereafter as PET/xPHB, where x is the mole fraction of the liquid-crystalline PHB.

Several investigations[2,7,11-15] had indicated the existence of at least two phases: a LC PHB-rich phase and a PET-rich phase. Scanning electron microscopy (SEM) results show the LC-rich phase as *islands* in the LC-poor matrix.[7] Phase transitions for different compositions have been studied by various laboratories around the world.[7,10-30] The results, however, are not uniform. Possible reasons for the differences between different laboratories are discussed in the beginning of section 8.

Despite the fairly large amounts of work expended on the PET/xPHB copolymers, a complete phase diagram was never constructed. To fully understand the multiphase character of the PET/xPHB copolyesters, the present work is focused on the phase diagram of thermal transitions temperatures (equilibrium and nonequilibrium) vs x, at constant atmospheric pressure. To construct the diagram, we shall use our own results obtained by several methods as well as results of other authors.

2. Experimental Procedures

Materials. We have studied pure PET and copolymer samples with $0.5 \leq x \leq 0.8$ produced by Eastman Kodak Co., Kingsport, TN; samples with $0.3 \leq x \leq 0.8$ synthesized by one of us in Duisburg following the procedure of Jackson and Kuhfuss;[10] LC-3000 of Unitika Ltd., Kyoto, which is PET/0.6PHB; samples with $x = 0.8$ were kindly provided to us by Prof. Lev Faitelson of the Institute of Polymer Mechanics of the Latvian Academy of Sciences, Riga, and synthesized by Prof. Vladilen Budtov and collaborators in St. Petersburg.[31]

Sample Preparation. Samples were dried for a minimum of 4 h and prepared by injection molding under the following conditions: temperatures in the barrel 270-280-290-300 °C; mold temperature 100 °C; filling pressure 130 J cm^{-3}; packing time 10 s; cooling time in the mold 10 s.

Measurements. *Dynamic Mechanical Thermal Analysis (DMTA).* Rectangular strips (8 mm × 8 mm × 1.5 mm) were analyzed in the bending mode in a Polymer Laboratories dynamic mechanical analyzer DMTA MK II, using single-cantilever clamping geometry, at frequencies ω = 3, 10, 30 Hz. These frequencies were chosen after earlier scans over wide frequency ranges. We used a constant strain that corresponds to a nominal peak-to-peak displacement of 64 μm. The temperature was varied from -100 to 100 °C; the heating rate was 2 K min^{-1}. Each composition was studied two or three times to prove the repeatability of the results; if all peak locations in two runs agreed within 3 K, a third run was not made; in either case, the averages of the transition temperatures as well as the entire ranges were recorded.

Differential Scanning Calorimetry (DSC). Calorimetric properties were investigated with a Perkin-Elmer DSC-7 apparatus. The samples were encapsulated in sealed aluminum pans and run under an atmosphere of circulating dry nitrogen. A heating rate of 20 K min^{-1} was set throughout the measurements. All transition temperatures reported here result from the second heating run and are the averages of three to five samples. The entire range of temperatures or each transition was recorded. Temperature calibration was performed with standard transition materials (indium and zinc).

† University of North Texas.
‡ Universität Duisburg.
§ Universidad de Antioquia.
® Abstract published in *Advance ACS Abstracts,* March 15, 1994.

0024-9297/94/2227-2262$04.50/0

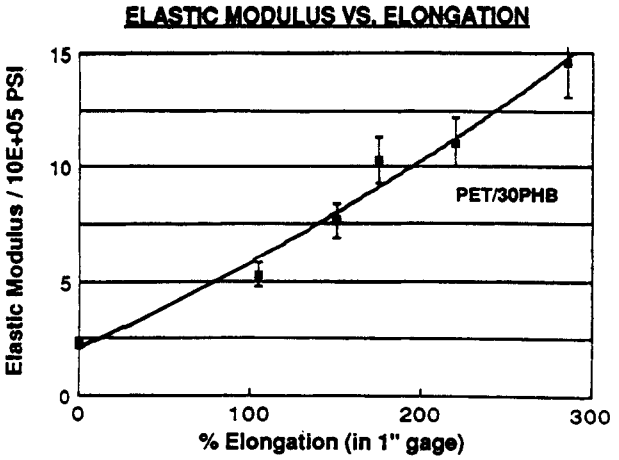

Figure 1. Elastic modulus changes at 25 °C resulting from cold drawing specimens of PET/0.3PHB. Filled squares represent each an average from five determinations.

Thermal Mechanical Analysis (TMA). Thermomechanical measurements of the samples were performed with a Perkin-Elmer thermomechanical analyzer TMA-7 in the penetration mode using a load of 200 mN. The temperature range was 30–320 °C, covered at a rate of 10 K min^{-1} in a helium atmosphere.

Cold Drawing and Tensile Testing. Cold drawing was performed at room temperature using 1-in. gage at $^3/_8$ in. min^{-1} (≈10 mm min^{-1}). Standards for such a procedure are not available. Tensile testing, including tensile modulus and tensile strength determination, was performed at the rate of 2 in. min^{-1} (≈51 mm min^{-1}); procedures defined by the ASTM D636 standard were followed.

3. Cold Drawing and Tensile Testing Results

The LC-rich islands observed by SEM microscopy are approximately spherical in shape.[7] We expected that the cold drawing should elongate the islands preferentially with respect to the LC-poor (PET-rich) matrix. We note, however, intrinsic polarized fluorescence intensity studies by Hennecke and co-workers[32–34] leading to the orientation coefficient as a function of the stretching ratio. While the fluorescence polarization signals are confined to the amorphous regions, the results for pure PET[33,34] show clearly an increase of the orientation coefficient with stretching.

We subjected to cold drawing specimens with $x = 0.3$ and subsequently determined in tension the elastic modulus and the tensile strength by the standard ASTM procedures. Since at this relatively low x value the islands are not numerous, evaluation of the mechanical reinforcement of the material by the LC sequences was particularly interesting. Needless to say, the formation and presence of the islands is reflected in the phase diagram, as discussed in section 8.

The results are shown respectively in Figures 1 and 2. (Standard American units are used, with 1 psi = 6895 Pa = 6.895×10^{-3} J cm^{-3}). It is evident that the cold drawing enhances both the elastic modulus and the tensile strength approximately 4-fold. Developing a theory of hierarchical structures,[2] we have performed wide-angle X-ray scattering (WAXS) diffractometry in HASYLAB at DESY, Hamburg, and combined the results with earlier SEM data.[7] Now we recall rule 4 of hierarchically structured materials:[2] since macroscopic properties are determined through *ascension* in the hierarchy, they are dependent on entities and their interactions at lower levels—in this case on the structures of the islands after deformation by cold drawing.

We have also studied effects of the LC concentration x on the elastic modulus and the tensile strength in the directions both along the flow (parallel) and perpendicular

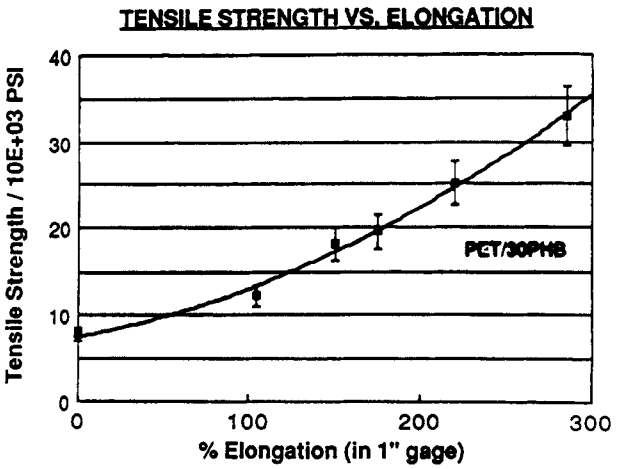

Figure 2. Tensile strength changes at 25 °C resulting from cold drawing specimens of PET/0.3PHB. Filled squares represent each an average from five determinations.

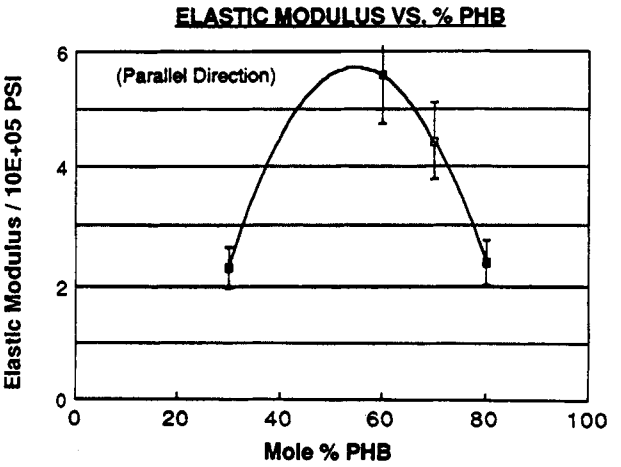

Figure 3. Elastic modulus of PET/xPHB copolymers as a function of x in the direction parallel to the flow during processing.

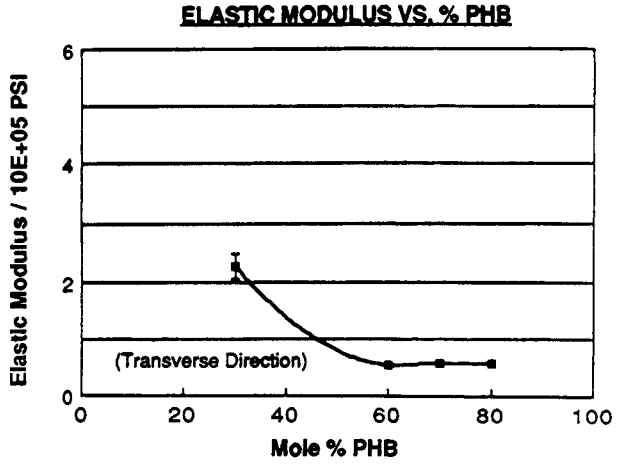

Figure 4. Elastic modulus of PET/xPHB copolymers as a function of x in the direction transverse to the flow during processing.

(transverse). The respective results are presented in Figures 3–6. We see how much orientation (as naturally caused by processing) influences the properties. In the transverse direction, increasing the LC concentration x in fact lowers both the elastic modulus and the tensile strength. In the parallel direction we have a maximum, resulting from the fact that for $x > 0.6$ the materials becomes progressively more brittle.

Our results agree with those of Heino and Seppälä,[35] who studied blends of an aromatic longitudinal HNA/xPHB, where HNA is 2,6-hydroxynaphthoic acid, with

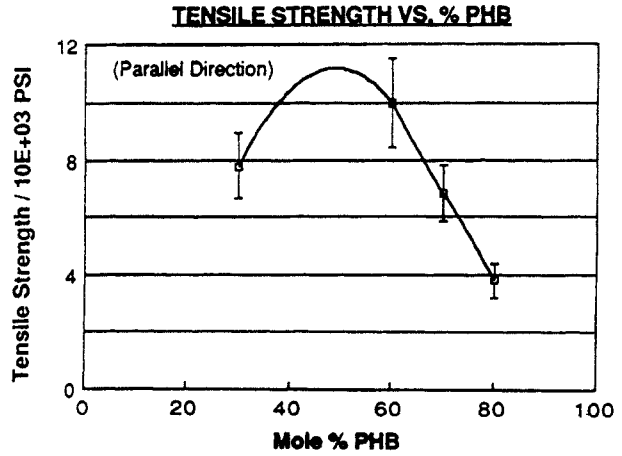

Figure 5. Tensile strength at 25 °C of PET/xPHB copolymers as a function of x in the direction parallel to flow during processing.

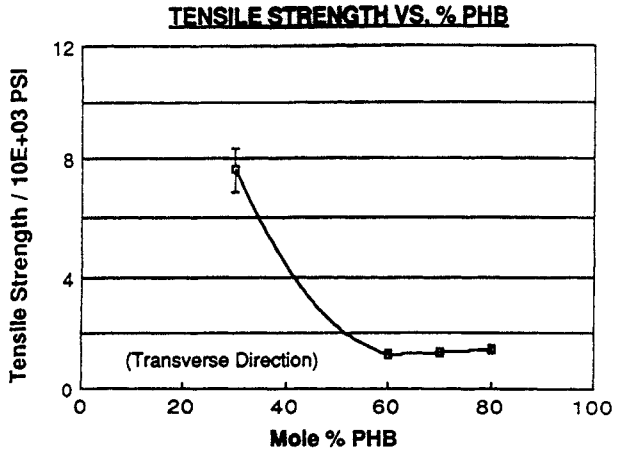

Figure 6. Tensile strength at 25 °C of PET/xPHB copolymers as a function of x in the direction transverse to flow during processing.

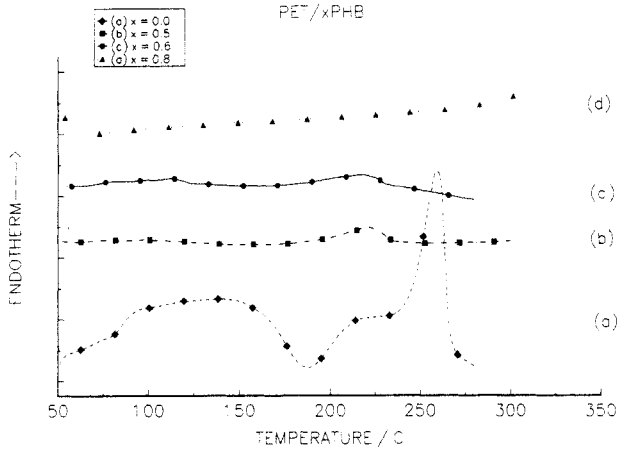

Figure 7. DSC scans for copolymers with varying x including $x = 0$.

poly(butylene terephthalate). Drawing after extrusion has also enhanced tensile strength and the elastic modulus, although not quite so much as in our pure PLC. As expected, Heino and Seppälä found the largest property enhancement for the highest PLC concentration they studied, confirming earlier results on HNA/PHB blends with other engineering polymers.[36,37]

4. DSC Results

In Figure 7 we present DSC scans for the PET/xPHB copolyesters, together with $x = 0$ (the PET sample). The glass transition temperature T_g is taken at the point where the half of the increase of heat capacity has occurred; note that some authors use the name α-transition instead of T_g.

Table 1. Transitions in PET/xPHB Copolymers As Determined by DSC

sample	T_g/°C	T_c/°C	T_m/°C	ΔH_f/J g^{-1}
PET	75	180	251	35.5
PET/0.5PHB	57	81	215	7.5
PET/0.6PHB	61	94	212	6.6
PET/0.8PHB			311	

The PET shows a T_g at about 75 °C and a crystalline melting transition T_m at about 251 °C. After annealing at 280 °C for 20 min, and quenching at 200 K min^{-1} to 30 °C, and holding at this temperature for 10 min, the crystallization temperature T_c appears around 180 °C, and the melting around 255 °C. PET/0.6PHB exhibits a T_g = 61 °C, lower than for PET, which agrees with prior results;[11,20] T_m (the melting points were taken as the temperature at the peak of the endotherm) is at 212 °C. Our calorimetric analysis exhibits only one glass transition for PET/0.5PHB, PET/0.6PHB, and PET/0.8PHB; the upper T_g value could not be identified. For PET/0.8PHB, probably due to the low concentration of PET, the heat flow during the phase separation process for the lower T_g is too small to verify the existence of this transition. The results from the DSC measurements are listed in Table 1. Other techniques *approximately* confirm the transition temperatures listed in the table. However, for reasons discussed in section 8, other techniques often give transition temperatures which agree better between themselves. In those cases these other values rather than DSC values are used in the construction of the phase diagram.

5. DMTA Results

DMTA scans for PET and PET/0.6PHB are shown respectively in parts a and b of Figure 8. For two constant frequencies ω, we show curves of the logarithmic storage modulus vs temperature, $\log(E'/\text{Pa})$ vs T, as well as curves of $\tan\delta = E''/E'$ vs T, where E'' is the loss modulus. Results for a third frequency, 10 kHz, have also been obtained but are not shown in Figure 8 so as to improve perspicuity.

The secondary relaxation temperatures T_β were taken as the peaks in $\tan\delta$ that appeared at $T < T_g$. We have observed this transition earlier by internal friction (IF) measurements,[24] and as noted then, it has been known for decades. Farrow et al.[38] have assigned it to some very restricted rotations of the glycol residues in PET; their conclusion was based on DMTA, nuclear magnetic resonance (NMR), infrared (IR) spectra, and x-ray diffractometry. Coburn and Boyd[39] have shown by dielectric relaxation (DER) that the β transition takes place in the amorphous phase only, since its strength goes down with increasing crystallinity. T_β centered around −60 °C for pure PET as found by IF agrees well with the log $E'(T)$ curve in Figure 8a, while the $\tan\delta(T)$ curve shows a very broad maximum, from around −65 °C or so up to approximately −40 °C.

For $x = 0.6$ the IF curves obtained on platinum as well on silica glass show the β transition centered around −50 °C.[24] Our log E' vs T curve in Figure 8b lends itself to the same interpretation, while the $\tan\delta(T)$ curve in the same figure shows the relaxational transition somewhat higher and also frequency dependent, with the maximum for ω = 3.0 Hz around −44 °C or so.

We defined the glass transition temperatures at the maximum of $\tan\delta$. The DMTA method is advantageous as compared to DSC in the location of the glass transition temperatures; large peaks in the loss modulus or $\tan\delta$ are

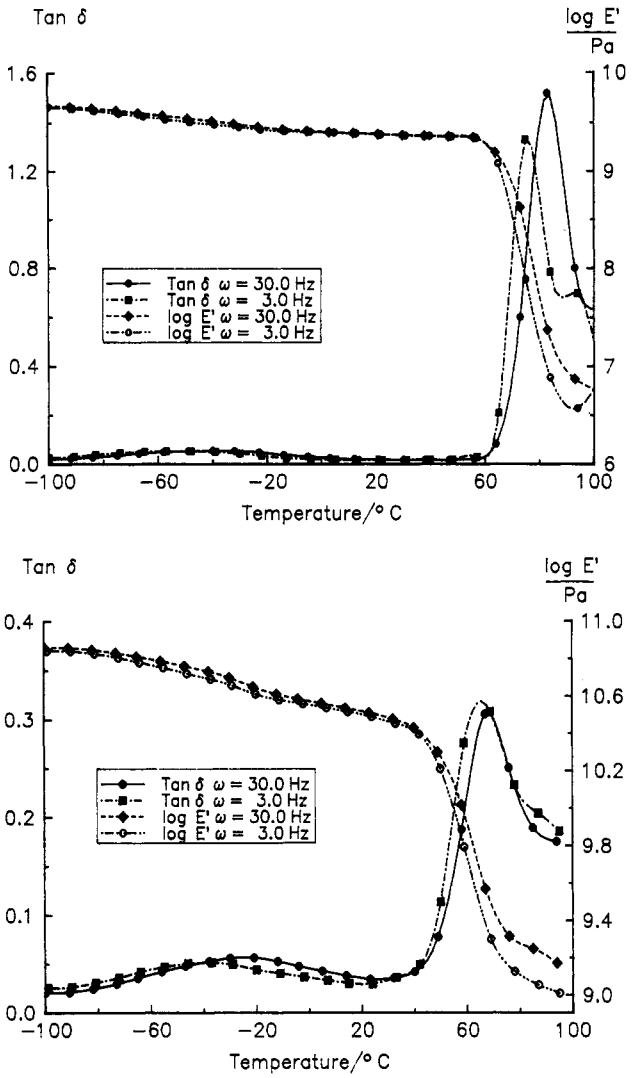

Figure 8. DMTA results for pure PET (a, top) and for PET/0.6PHB (b, bottom).

observed, as compared to small steps in the DSC curve around T_g. Lower frequencies are closer to the equilibrium state, and indeed we find that the glass transition temperatures measured at 3 or 10 Hz are very similar to those obtained by DSC; at the higher frequency of 30 Hz the values for T_g are somewhat higher. At 3 Hz we find T_g for PET at 77 °C and for PET/0.6PHB at 65 °C.

Since transesterification reactions are known to occur in polyesters, the following needs to be noted. ^{13}C NMR spectroscopic studies by Kosfeld, one of us, and Friedrich[40] show that such reactions take time, and measurable effects are observed at temperatures exceeding 270 °C. In fact, transesterification tends to promote random statistical distribution of PET and PHB sequences, and Guan and co-workers[41] found by ^1H NMR at 400 MHz that samples kept at the temperature of 270 °C do *not* show random distribution, while those kept at 290 °C are closer to that distribution. An overwhelming majority of the transitions studied by us takes place at temperatures lower than 290 °C.

6. TMA Results

TMA scans for PET/0.5PHB, PET/0.6PHB, and PET/0.8PHB are shown respectively in parts a–c of Figure 9. The penetration of a quartz rod with a flat tip under small load gives an additional, independent information which very often appeared to be essential for proper interpretation of the results obtained from the other methods

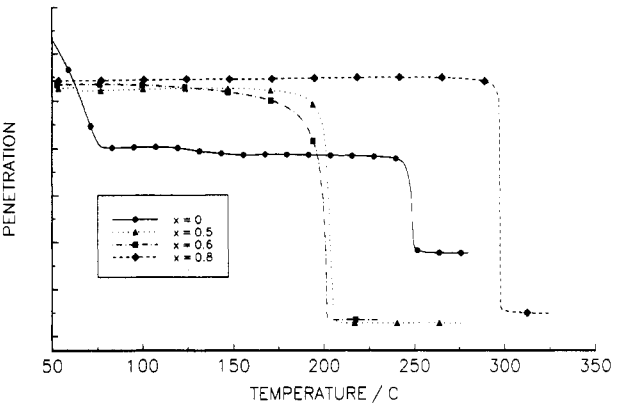

Figure 9. TMA results for PET/xPHB copolymers including x = 0.

mentioned above. TMA helps to confirm the results obtained by other methods.

7. Phase Structures, Phase Diagram, and Intelligent Processing Connection

Properties of materials, polymeric or otherwise, are of course determined by chemical composition as well as by structures produced during processing. For PLCs the situation is *more difficult* than for engineering polymers; we know already from the first paper by Jackson and Kuhfuss[10] how easily PLCs acquire orientation during processing; high anisotropy of properties ensues. While in some cases the anisotropy is desirable, controlling the resulting properties is possible only if we have sufficient knowledge of morphologies and phase structures and also if we can locate each structure in the corresponding region of the phase diagram.

There has been some prior and interesting work on processing of the PLCs and their blends, such as the suggestion of Golovoy and co-workers[42] to enhance fibrillar structures in injection molding by machining fine grooves in the mold runners. Seppälä and co-workers[35–37] have found that extrusion enhances mechanical properties of the PLC-containing blends beyond those of injection-molded specimen, apparently because additional drawing occurs. Our particular approach consists in the determination of the appropriate phase diagram first and defining processing conditions only afterward. We call this approach *intelligent processing*. In the present paper we define some peculiarities of phase diagrams of PLC-containing systems, on the basis of a specific example.

It is customary to show in phase diagrams equilibrium phases only. However, as already discussed,[5] we believe that in general nonequilibrium phases have to be included in the PLC phase diagrams. Some such phases, at low temperatures in particular, exhibit *high longevity*, apparently because of the presence of rigid constituents; disregarding them would have obvious consequences for processing procedures and for the properties of the products. Moreover, from the behavior of the glass transition temperatures, conclusions can be drawn on the miscibility of the constituents.

The idea of inclusion of nonequilibrium phases in PLC phase diagrams appears to be reinforced by results of Springer and co-workers[43–45] on comb PLCs. One of these polymers undergoes a transition from a metastable monolayer smectic A phase into bilayer smectic C phase, but only after annealing *above* a certain temperature.[43] The same group has found several cases of polymorphism in smectic phases.[44,45]

8. PET/xPHB Phase Diagram

The phase diagram of pure PET/xPHB copolymers (no blends) as a function of x resulting from different methods and different authors is shown in Figure 10. *Nonequilibrium* phases and the corresponding transitions and also the relaxational transition β discussed in section 5 are included.

Analyzing results of earlier investigators, we have noticed some differences between different sources. There are several reasons for this. First, not in all cases the procedures used to locate a transition temperature (maximum of a peak, midpoint of the temperature range over which a transition occurs) are specified. However, any prejudgement on our part—such as arbitrary elimination of some of the extant points—would be wrong. Second, various synthesis procedures do not necessarily produce the same degree of randomness in the incorporation of PET and PHB sequences into the copolymer chains. Third, thermal histories of the samples—typically strongly dependent on procedures and conditions—might be different. Interesting in this context is a series of papers by Tomka and co-workers[46-49] on PLCs (including terpolymers) in which compositions, processing (fiber formation), heat treatment (or lack of it) and presence (or absence) of a catalyst or strong acid were all used to manipulate the crystallinity, morphology, and processing windows of the materials. Somewhat similarly, Schmack and Vogel[50] have found that annealing alone affects considerably the maxima of melt peak temperatures in DSC runs, as well the resulting crystallinity and morphology. And fourth, differences in molar mass distributions also play a role. To ensure comparability, the $\bar{M}$ averages should be the same, the $\bar{M}$ distributions the same, and the chain statistics at least comparable.

Even when the chemical composition, degree of randomness along the chain, thermal history, etc., are the same, some differences between transition-locations-determined techniques might still appear, depending on the amount and size of the domains investigated. The domain size has an influence on the resolution of neighboring signals, their peak width, and temperature of the glass transition if the size of the glassy domains is beyond a certain dimension.[51,52] The minimal domain size detectable by DMTA is assumed to be between 1.5 and 15 nm.[53-56] This is at the overlap of wide-angle X-ray scattering (WAXS, 0.1–2 nm) and small-angle X-ray scattering (SAXS, 1.0–100 nm). SEM may resolve sizes down to 10 nm. As for DSC, DER, and TMA, there seem to be no values of minimal domain size available in literature. However, this size is expected to be larger than for DMTA.

Given the difficulties discussed above, we had to define and follow several procedures to arrive at a reliable phase diagram. First, we have studied materials synthesized by a single procedure, namely, developed by Eastman Kodak Co., thus eliminating the problems with the statistics of sequence distribution along the chains and with the molecular mass distributions. Second, in the present work we used results obtained earlier by thermally stimulated depolarization (TSD),[23] SEM,[7] WAXS,[2] and also internal friction (IF)[24] for the same materials, with researchers in several countries on three continents thus involved in the project. Third, including results from the literature, we have gathered results obtained by DSC, DMTA, TMA, TSD, IF, and DER, plus structural and mobility studies with SEM, WAXS, SAXS, NMR, and IR. Fourth, several techniques were applied to identical samples at different locations (Denton, Duisburg). Fifth, we have created a series of very large-scale phase diagrams on which each transition determined by a single technique at a single location was represented by a *range* rather than a point—if only a range was available. The ranges show better overlaps than the points, but cannot be shown without causing confusion on the phase diagram below (Figure 10).

In defining the transition temperatures for the diagram, much weight was given when the same temperatures was obtained from different types of experiments or else from a single type of experiment but conducted in different laboratories. DSC often provides broad transition ranges such that the maximum of the peaks is hard to locate. Moreover, thermal effects accompanying transitions involving LC phases are smaller than in non-LC materials (melting into an isotropic phase causes larger structure changes than the melting into an LC phase). By contrast—as discussed in section 6—DMTA results show relatively large peaks. In the case of a conflict between a DSC result and results from other techniques, the DSC result was given the lower weight. As briefly mentioned in section 6, TMA turned out to be particularly trustworthy; transitions seen by any other technique typically show up in TMA. Further, drawing a line in the phase diagram for a given transition as a function of composition provided an additional check; while transition temperatures were determined independently for each concentration for which data were available, "wavy" transition lines were not obtained. Finally, we took into account the classic thermodynamic phase rule due to Gibbs[57] and its application to polymer phase diagrams as discussed by Koningsveld and Berghmans.[58]

Inspection of Figure 10 shows the complexity of the phase diagram, still higher than that of the PLC system studied by Zachmann and collaborators,[9] namely, copolymers of poly(ethylenenaphthalene-2,6-dicarboxylate (PEN) with PHB. One reason for the additional complexity is the inclusion of relaxational transitions (β and α) and the deliberate inclusion of nonequilibrium phases. Continuous lines correspond to localized transitions or relaxations, such that the number of experimental points is adequate for reasonably accurate inferences. The nearly horizontal dotted line represents approximately the *maximum* of the cold crystallization rate; the process occurs of course also below and above the line. The nearly vertical dotted line represents the phase separation related to creation of LC-rich islands (a eutectic-like diagram); here also a region on both sides of the dotted line is involved. The line is not quite vertical, because the statistical-mechanical theory of Flory and Matheson[59,60] as amplified in refs 61 and 62 shows that at lower temperatures an orientationally ordered (LC-rich) phase appears at lower LC concentrations θ. Since we have two-constituents copolymers only, θ in ref 61 is equal to x in this paper. The broken lines in the diagram pertain to the part of the diagram where the line location is known less accurately because of the low density of experimental points (related to thermal degradation at longer times). Calculations based on the theory[61] will be made for the LC-i coexistence line in that region.

The regions in the diagram marked with Roman numbers contain the following phases: (I) PET crystals, isotropic glass (PET matrix with some PHB sequences), both below solid-state β relaxations; (II) PET crystals, PHB-rich islands, isotropic (PET-rich) glass, PHB-rich glass, all below solid-state β relaxations; (III) PET crystals, isotropic (PET-rich) glass, both above solid-state β relaxation transition; (IV) PET crystals, PHB-rich islands, isotropic PET-rich glass, PHB-rich glass, all above β

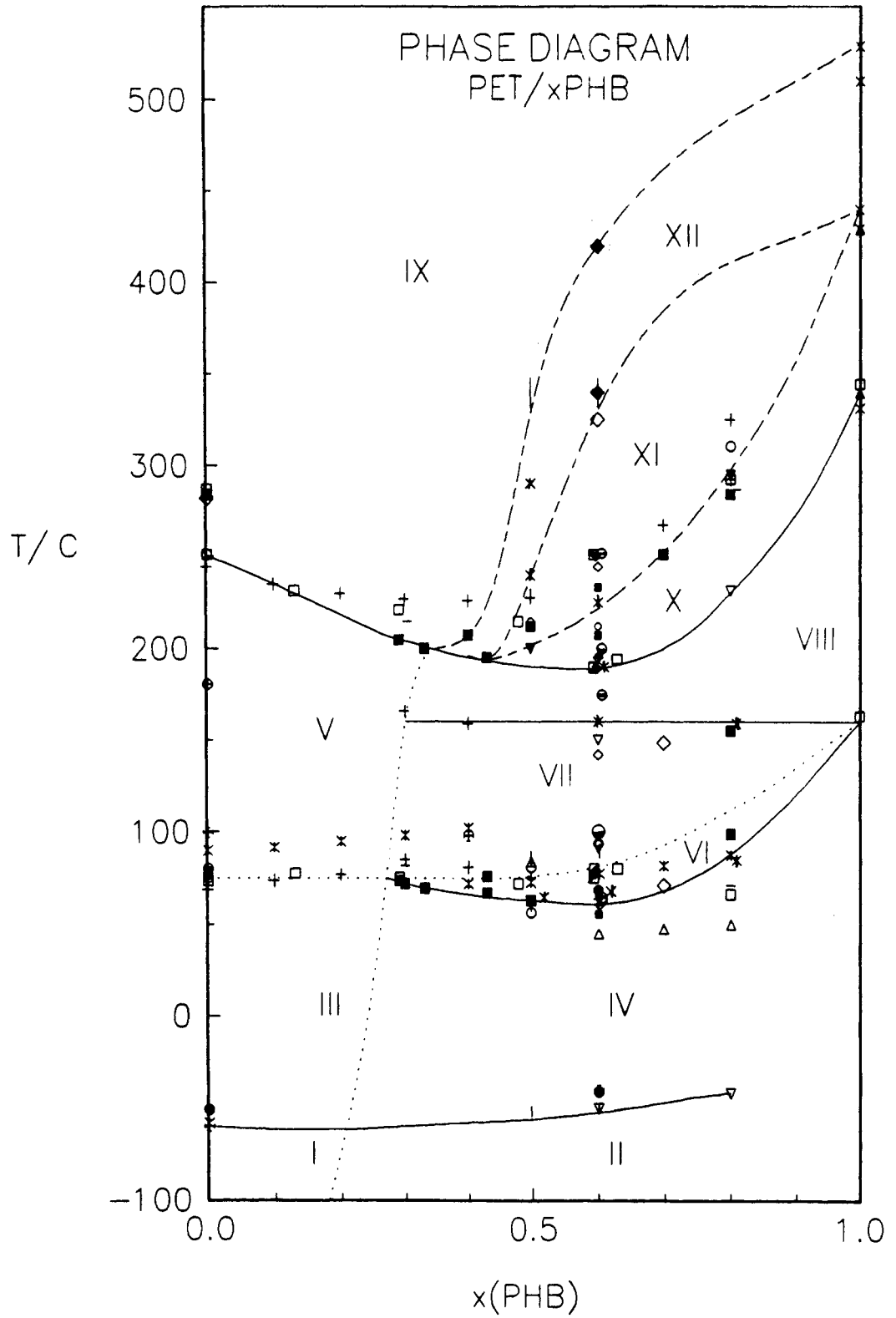

Figure 10. Equilibrium and nonequilibrium phase diagram of PET/xPHB copolymers in the temperature vs x coordinates; see text. The symbols of the diagram correspond to the following sources: (○) our results (DSC); (●) our results (DMTA); (▼) our results (TMA in Denton); (■) our results (representing jointly results obtained by TMA, and pendulum-type DMTA and DSC in Duisburg); (*) our results (Gnomix volume–pressure–temperature apparatus); (+) Jackson, Jr., W. J.; Kuhfuss, H. F. (DSC, DMTA);[10] (⊖) Menczel, J.; Wunderlich, B. (DSC);[11] (□) Meesiri, W.; Menczel, J.; Gaur, U.; Wunderlich, B. (DSC);[12] (◇) Sun, T.; Porter, R. S. (DSC, DMTA, OT, OM);[15] (◈) Jeziorny, A. (DSC);[16] (▣) Zhou, Ch.; Clough, S. B. (DSC);[17] (◆) Viney, C.; Windle, A. H. (DSC, OM);[18] (△) Benson, R. S.; Lewis, D. N. (DMTA);[19] (▽) Gedde, U. W.; Burger, D.; Boyd, R. H. (DER);[20] (×) Kricheldorf, H. R.; Schwarz, G. (DSC, WAXS, OM);[21] (⧗) Chen, D.; Zachmann, H. G. (DSC, DMTA);[22] (◒) Brostow, W.; Kaushik, B.; Mall, S.; Talwar, I. (TSD);[23] (|) Brostow, W.; Samatowicz, D. (IF);[24] (–) Zhuang, P.; Kyu, T.; White, J. L. (DSC);[26] (⧺) Takase, Y.; Mitchell, G. R.; Odajima, A. (DER);[27] (▲) Yoon, D. Y.; et al. (DSC, DER);[28] (⧄) Joseph, E.; Wilkes, G. L.; Baird, D. G. (DSC);[29] (⧈) Cuculo, J. A.; Chen, G. Y. (DSC).[30] OT = optical transmission; DER = dielectrical relaxation; DMTA = dynamic mechanical thermal analysis; OM = optical microscopic; TMA = thermomechanical analysis; IF = internal friction; TSD = thermally stimulated depolarization; DSC = differential scanning calorimetry; WAXS = wide-angle X-ray scattering.

relaxation; (V) PET crystals, quasi-liquid; (VI) and (VII) PET crystals, PHB-rich islands, PHB-rich glass, quasi-liquid; (VIII) PET crystals, PHB-rich islands, quasi-liquid; (IX) isotropic liquid; (X) smectic E, isotropic liquid; (XI)

smectic E, smectic B, isotropic liquid; (XII) smectic B, isotropic liquid.

Coexistence of two smectic phases in region XI is worth noting. While clear on thermodynamic grounds, it was supposed to be more typical for monomeric liquid crystals (MLCs). However, Galli and co-workers[63] argue that the phenomenon of the mesophase coexistence might be more frequent in PLCs than hitherto believed.

For our assignments of the phases and transitions in the copolymers particularly useful were the results of Kricheldorf and Schwarz[21] and Yoon and co-workers[28] on pure PHB. The independence of the glass transition of the PET from x for low x values (below the $\theta_{LC\ limit}$) indicates that the solubility of PHB in the PET-rich phase is quite low, while the PHB-rich phase allows relatively higher concentrations of PET. Here $\theta_{LC\ limit}$ is the lowest concentration θ of the LC component at which islands of the LC-rich phase can be formed; see Figure 7 in ref 61. The existence of $\theta_{LC\ limit}$ is particularly important for the mechanical reinforcement of the polymer by the LC sequences. Kyotani and co-workers[64] have found no improvement of tensile properties for PLC-containing blends with $\theta < 0.05$, which is clearly below the $\theta_{LC\ limit}$. Their WAXS studies show formation of the islands, spherical or elliptical, also above a certain θ threshold. Their longitudinal PLC (containing PHB but different than ours) shows in WAXS an increase in orientation with an increased draw ratio, in agreement with our results above in section 3.

The quasi-liquid phase existing in several phase regions defined above will be discussed in the following section.

9. Quasi-Liquid Phase

The diagram in Figure 10 contains a phase such that its existence has been noted in earlier PLC work, namely, the *quasi-liquid* (q-l).[1,2] This is the material which was in the amorphous state below its glass transition but now is in the temperature range between T_g and the melting transition (which can be a transition into a mesophase). Except for elastomers, when one then talks about the *leathery* state, one calls such materials simply liquids. However, in the case of the PLCs in particular, that name is *not* appropriate for several reasons:

(i) The quasi-liquid phase does *not* exhibit the ordinary liquid mobility. The presence of another component below its glass transition and/or of crystallites prevents the phase from flowing like a liquid does. This in contrast to non-LC polymers between T_g and T_m, where the formerly amorphous phase flows around the crystalline regions, with the liquid viscosity dependent for all purposes only on the temperature. The concentration of the quasi-liquid depends also on the concentration of LC sequences. In this context, we note the deuteron NMR results of Zachman and collaborators,[9] who have found that in PET/xPHB copolymers the PHB sequences *decrease considerably* the mobility of PET sequences.

(ii) The notion of a "liquid" brings about a mental association of a material which upon heating can only undergo vaporization or, if it is a polymer melt, no further transition at all. By contrast, the material containing a q-l phase has to undergo at least two more phase transitions: melting and isotropization at the clearing point. If more than one liquid-crystalline phase is formed, say smectic C and nematic, then there will be even more transitions.

(iii) It is in the quasi-liquid phase that the process of the so-called "cold crystallization" can occur.

(iv) Finally, and as briefly noted above, q-l shows an analogy with the leathery state in elastomers. Both types of systems are immediately above their glass transition regions, and both exhibit *retarded* reactions to application of external forces.

10. Some Concluding Remarks

In Figure 10 we see multiplicity of phase transitions of the LC component, limited miscibility discussed already in section 8, a large number of regions, and typically several phases in each region. This complexity of the phase diagram is a consequence of several factors. Primordial here is the relative rigidity of LC sequences, producing orientation even in weak shearing or other (electric or magnetic) fields, and the orientation-induced interactions. We study these effects also by amplifying[61,62,65] the Flory–Matheson statistical-mechanical theory[59,60] of rigid-rod containing systems, by molecular dynamics computers simulations of the PLC systems subjected to external mechanical forces,[66] and also by development of rules based on the concept of homeomorphism pertaining to relations in hierarchical structures.[2] We believe that a satisfactory understanding of the structure–property relationships in PLC systems can be acquired only *concomitantly* from the approaches named above plus experiments conducted by a variety of techniques. As an example, Zachman, Linder, and co-workers[67] used small-angle neutron scattering (SANS) to determine the average length η of the LC sequences in PET/xPHB chains for x = 0.6, 0.7, 0.8. η is an important parameter in statistical mechanics of PLC systems.[59–62,65]

While we are stressing the complexity, we are dealing here with pure PLCs. PLC-containing blends, and their phase diagrams will not necessarily be simpler.[68] PLC-containing solutions involve additional challenges, as shown by light-scattering and other measurements on simple PLC combs by Fritz and Springer.[69] They found that the stiffness of the LC sequences varies also with the concentration in solution. Finally, we note the work of Kricheldorf[70] postulating that not only steric factors such as stiffness but also electric interactions are essential in the formation of LC phases.

Acknowledgment. Mr. Stephen H. Saboe, Jr., formerly at Drexel University, Philadelphia, and now with E. I duPont de Nemours, Webster, TX, has participated in the experimental work. So did Dr. Frank Schubert, formerly at the University of Duisburg, now with Bakelite, Duisburg. The technical support of HASYLAB (Hamburger Synchrotron Laboratorium) at DESY (Deutsches Elektronen Synchrotron) in X-ray diffractometry is appreciated. We benefitted from discussions with a number of colleagues: Prof. Georg Hinrichsen and Prof. Jürgen Springer, Technische Universität Berlin; Prof. Hans R. Kricheldorf and Prof. Gerhard Zachmann, Universität Hamburg; Dr. Joachim Gähde, Zentrum für Makromolekulare Chemie, Berlin-Adlershof; Prof. Lev Faitelson and Prof. Robert Maksimov, Poliméru Mehánikas Institúts, Latvijas Zinátnu Akadémija, Riga. Prof. Jukka Seppälä and Mr. Markku Heino, Helsinki University of Technology, have kindly provided comments on the manuscript. Financial support was provided by the Robert A. Welch Foundation, Houston (Grant B-1203), by the Deutsche Forschungsgemeinschaft, Bonn (to M.H.), and by the University of North Texas (to B.L.L.).

References and Notes

(1) Brostow, W.; Dziemianowicz, T. S.; Hess, M.; Kosfeld, R. *Mater. Res. Soc. Symp.* **1990**, *171*, 177.

(2) Brostow, W.; Hess, M. *Mater. Res. Soc. Symp.* **1992**, *255*, 57.
(3) Brostow, W. *Kunststoffe* **1988**, *78*, 411.
(4) Witt, W. *Kunststoffe* **1988**, *78*, 795.
(5) Brostow, W. *Polymer* **1990**, *31*, 979.
(6) Brostow, W. In *Liquid Crystalline Polymers: From Structures to Applications*. Collyer, A. A., Ed.; Elsevier Applied Science: London, 1992; Chapter 1.
(7) Brostow, W.; Dziemianowicz, T.; Romanski, J.; Werber, W. *Polym. Eng. Sci.* **1988**, *28*, 785.
(8) Brostow, W. In *Fifth Israel Materials Engineering Conference*; Bamberger M., Shorr, M., Eds.; Freund Publishing House: London, 1991; p 219.
(9) Buchner, S.; Chen, D.; Gehrke, R.; Zachmann, H. G. *Mol. Cryst. Liq. Cryst.* **1988**, *155*, 357.
(10) Jackson, Jr. W. J.; Kuhfuss, H. F. *J. Polym. Sci. Phys.* **1976**, *14*, 2043.
(11) Menczel, J.; Wunderlich, B. *J. Polym. Sci. Polym. Phys. Ed.* **1980**, *18*, 1433.
(12) Meesiri, W.; Menczel, J.; Gaur, U.; Wunderlich, B. *J. Polym. Sci. Phys.* **1982**, *20*, 719.
(13) Uzman, M.; Kühnpast, K.; Springer, *J. Makromol. Chem.* **1989**, *190*, 3185.
(14) Kwiatkowski, M.; Hinrichsen, G. *J. Mater. Sci.* **1990**, *25*, 1548.
(15) Sun, T.; Porter, R. S. *Polym. Commun.* **1990**, *31*, 70.
(16) Jeziorny, A. *Polimery* **1989**, *34*, 210.
(17) Zhou, Ch.; Clough, S. B. *Polym. Eng. Sci.* **1988**, *28*, 65.
(18) Viney, C.; Windle, A. H. *J. Mater. Sci.* **1982**, *17*, 2661.
(19) Benson, R. S.; Lewis, D. N. *Polym. Commun.* **1987**, *28*, 289.
(20) Gedde, U. W.; Burger, D.; Boyd, R. H. *Macromolecules* **1987**, *20*, 988.
(21) Kricheldorf, H. R.; Schwarz, G. *Polymer* **1990**, *31*, 481.
(22) Chen, D.; Zachmann, H. G. *Polymer* **1991**, *32*, 1612.
(23) Brostow, W.; Kaushik, B.; Mall, S.; Talwar, I. *Polymer* **1992**, *33*, 4687.
(24) Brostow, W.; Samatowicz, D. *Polymer Eng. Sci.* **1993**, *33*, 581.
(25) Zachariades, A. E.; Economy, J.; Logan, J. A. *J. Appl. Polym. Sci.* **1982**, *27*, 2009.
(26) Zhuang, P.; Kyu, T.; White, J. L. *Polym. Eng. Sci.* **1988**, *28*, 1095.
(27) Takase, Y.; Mitchell, G. R.; Odajima, A. *Polym. Commun.* **1986**, *27*, 76.
(28) Yoon, D. Y.; Masciocchi, N.; Depero, L. E.; Viney, C.; Parrish, W. *Macromolecules* **1990**, *23*, 1793.
(29) Joseph, E.; Wilkes, G. L.; Baird, D. G. *Polymer* **1985**, *26*, 689.
(30) Cuculo, J. A.; Chen, G. Y. *J. Polym. Sci. Phys.* **1988**, *26*, 179.
(31) Faitelson, L., private communication, June 1993.
(32) Hennecke, M. H. *J. Polym. Sci. Phys.* **1986**, *24*, 111.
(33) Hennecke, M. H.; Kud, A.; Kurz, K.; Fuhrmann, J. *Colloid Polym. Sci.* **1987**, *265*, 674.
(34) Hennecke, M. H.; Kurz, K.; Fuhrmann, J. *Macromolecules* **1992**, *25*, 6190.
(35) Heino, M. T.; Seppälä, J. V. *Polym. Bull.* **1993**, *30*, 353.
(36) Seppälä, J.; Heino, M. T.; Kupanen, C. *J. Appl. Polym. Sci.* **1992**, *44*, 1051.
(37) Heino, M. T.; Seppälä, J. V. *J. Appl. Polym. Sci.* **1992**, *44*, 2185.
(38) Farrow, G.; McIntyre, J.; Ward, I. M. *Makromol. Chem.* **1960**, *38*, 147.
(39) Coburn, J. C.; Boyd, R. H. *Macromolecules* **1986**, *19*, 2238.
(40) Kosfeld, R.; Hess, M.; Friedrich, K. *Mater. Chem. Phys.* **1987**, *18*, 93.
(41) Guan, G.; Wang, H.; Chung, Y.; Zhou, H.; Sun, T. *J. China Text. Univer.* **1991**, *17* (3), 1. Quoted after: *Refer. Zh. Khim. VMS* **1992**, *10C*, 19.
(42) Golovoy, A.; Kozlowski, M.; Narkis, M. *Polym. Eng. Sci.* **1992**, *32*, 854.
(43) Wolff, D.; Cackovic, C.; Krüger, H.; Rübner, J.; Springer, J. *Liq. Cryst.* **1993**, *14*, 917.
(44) Kühnpast, K.; Springer, J.; Scherowsky, G.; Giesselmann, F.; Zugenmaier, P. *Liq. Cryst.* **1993**, *14*, 861.
(45) Davidson, P.; Kühnpast, K.; Springer, J.; Scherowsky, G. *Liq. Cryst.* **1993**, *14*, 901.
(46) Li, Z. G.; McIntyre, J. E.; Tomka, J. G. *Polymer* **1993**, *34*, 551.
(47) Cao, J.; Karayannidis, G.; McIntyre, J. E.; Tomka, J. G. *Polymer* **1993**, *34*, 1471.
(48) Johnson, D. J.; Karacan, I.; Tomka, J. G. *Polymer* **1993**, *34*, 1749.
(49) Li, Z. G.; McIntyre, J. G.; Tomka, J. G.; Voice, A. M. *Polymer* **1993**, *34*, 1946.
(50) Schmack, G.; Vogel, R. *Kunststoffe* **1992**, *82*, 1011.
(51) Bares, J. *Macromolecules* **1975**, *8*, 244.
(52) Wetton, R. E.; Moore, J. D.; Ingram, P. *Polymer* **1973**, *14*, 161.
(53) Stoelting, J.; Karasz, F. E.; McKnight, W. J. *Polym. Eng. Sci.* **1970**, *10*, 133.
(54) Garton, A. *Polym. Eng. Sci.* **1982**, *22*, 124.
(55) Vinogradov, Ya. L.; Martinov, M. A.; Olshanik, G. A. *Polym. Sci. USSR* **1975**, *7*, 1605.
(56) Hammer, C. F. *Macromolecules* **1971**, *4*, 347.
(57) Gibbs, J. W. *The Scientific Papers*; Dover Reprint: Mineola, NY, 1961; Vol. 1, Thermodynamics.
(58) Koningsveld, R.; Berghmans, H. In *Transitions in Oligomer and Polymer Systems*; Bethge, K., Ed.; European Physical Society: Geneva 1993.
(59) Flory, P. J. *Proc. R. Soc. A* **1956**, *234*, *60*, 73.
(60) Matheson, R. R., Jr.; Flory, P. J. *Macromolecules* **1981**, *14*, 954.
(61) Jonah, D. A.; Brostow, W.; Hess, M. *Macromolecules* **1993**, *26*, 76.
(62) Brostow, W.; Walasek, J. *Macromolecules*, in press.
(63) Galli, G.; Chiellini, E.; Laus, M.; Angeloni, A. S.; Francescangeli, O.; Yang, B. *Macromolecules* **1994**, *27*, 303.
(64) Kyotani, M.; Kaito, A.; Nakayanna, K. *Polymer* **1992**, *33*, 4756.
(65) Blonski, S.; Brostow, W.; Jonah, D. A.; Hess, M. *Macromolecules* **1993**, *26*, 84.
(66) Blonski, S.; Brostow, W. *J. Chem. Phys.* **1991**, *95*, 2890.
(67) Olbrich, E.; Chen, D.; Zachmann, H. G.; Lindner, P. *Macromolecules* **1991**, *24*, 4364.
(68) Brostow, W.; Hess, M.; López, B. L.; Sterzynski, T., manuscript in preparation.
(69) Fritz, L.; Springer, *Makromol. Chem.* **1993**, *194*, 2047.
(70) Kricheldorf, H. R. *Mol. Cryst. Liq. Cryst.*, in press (preprint from the University of Hamburg).